Toward high recovery and selective leaching of zinc from electric arc furnace dust with different physicochemical properties

Han Saem Lee[1], Da So Mi Park[2], Yuhoon Hwang[2], Jong Gil Ha[3], Hyung Sang Shin[1†]

[1]Department of Environmental Energy Engineering, Seoul National University of Science and Technology, Seoul 01811, Republic of Korea
[2]Department of Environmental Engineering, Seoul National University of Science and Technology, Seoul 01811, Republic of Korea
[3]Jeongsoo New Technology, LTD., Seoul 02792, Republic of Korea

ABSTRACT

This work describes highly efficient recovery and selective leaching of Zn from electric arc furnace dust (EAFD) with different physicochemical properties, induced by acid leaching at ambient conditions. The chemical compositions, mineralogical phases, and particle sizes of the EAFDs were analyzed and compared. The effects of leaching time, liquid/solid ratio, acid type, and acid concentration on the selective leaching of Zn were also studied. The EAFD with high Fe/Zn ratio (> 1, EAFD$_3$) was richer in ZnFe$_2$O$_4$ and exhibited larger particle size than samples with low Fe/Zn ratio (< 1, EAFD$_{1,2}$). ANOVA analysis revealed that the Fe/Zn ratios of the EAFDs also have a significant effect on Zn extraction ($p < 0.005$). Selective leaching of Zn with minimum Fe dissolution was obtained at pH > 4.5, regardless of other parameters or sample properties. The maximum Zn extraction rate obtained by the pH control was over 97% for EAFD$_1$ and EAFD$_2$, 76% for EAFD$_3$, and 80% for EAFD$_4$. The present results confirm that the Fe/Zn ratio can be used to identify EAFDs that permits facile and high-yield Zn recovery, and pH can be used as a process control factor for selective leaching of Zn regardless of any differences in the properties of the EAFD sample.

Keywords: Acid leaching, Electric arc furnace dust, pH, Physicochemical characteristics, Zinc leaching

1. Introduction

Electric arc furnace dust (EAFD) is the solid waste recovered from dust collectors [1]. Approximately 10-30 kg of EAFD is produced per ton of steel [2]. EAFD is considered a hazardous waste because unsafe metals (e.g., lead and cadmium) [3] may have been incorporated during the steelmaking process or used as alloying elements and plated onto steel scraps [4]. EAFD usually contains 10-50 wt% of Zn, which can be used as high-value products [4]. Hence, EAFD has been actively recycled to recover Zn. Zn extraction from EAFD may also allow reuse of residues as raw materials for steelmaking and reduce the quantity of EAFD left for disposal [5, 6].

The pyrometallurgical method, which is a dry process, is only suitable for high-volume EAFD recycling owing to high initial investment and operational costs [5]. The hydrometallurgical method using alkali or acid has attracted significant attention over the last decade. In particular, the acid-based wet process affords a high Zn recovery rate by using high temperatures, pressures,

or acid concentrations, and has lower operating costs than the alkali wet process [1-4]. High Zn recoveries of 92% [7] and > 97% [8] have been achieved using various acid leaching processes. However, as the recovery of Zn is highly dependent on the EAFD characteristics, such as the ferrite content and particle size, ensuring consistent recovery yields is challenging. As each EAFD has different properties, specifying appropriate process conditions for Zn recovery by acid leaching is difficult [5, 9]. Only a few studies have analyzed the different features of various types of EAFDs and the effect of their distinctive characteristics on Zn recovery [10]. Consequently, an acid leaching process has not been widely commercialized and there are no available methods for selecting EAFDs showed consistently high Zn recovery yields. Thus, there is a need to develop a method that enables the selection of suitable EAFDs for the recycling processes by considering the characteristics of the samples. Although higher Zn ferrite (ZnFe$_2$O$_4$, franklinite) contents in the EAFD are known to make Zn recovery more difficult [8, 9], there is no known method for easily estimating the amount of ZnFe$_2$O$_4$ in the EAFD during recovery by acid leaching [11].

Therefore, it is important to determine specific properties that make an EAFD suitable for efficient acid leaching and need a selecting factor with detailed criterion for choosing an appropriate EAFD in the acid leaching process.

Another disadvantage of the acid leaching process is the simultaneous leaching of Fe with Zn [5]. Among the various forms of Zn in EAFDs [3, 6], $ZnFe_2O_4$ is highly resistant to dissolution under normal acid leaching conditions. Therefore, Zn recovery from $ZnFe_2O_4$ has required harsher conditions, including high temperatures, high pressures, and high acid concentrations during leaching [12]. However, these methods suffer from large amounts of Fe leaching and high energy costs. It is therefore highly desirable to develop an acid leaching technique with improved Zn recovery without Fe and low energy consumption [6]. Crystallization, ion exchange, solvent extraction, and oxidation followed by precipitation are all effective for controlling Fe leaching or removing leached Fe via a wet-acid process [13, 14]. Although these previous methods increased the removal efficiency of Fe, they still required high temperatures and pressures, consumed significant energy, and required an additional step to separate Zn and Fe. The precipitation method using pH for removing Fe from leaching solution has been reported to have good separation efficiency and no additional step in previous studies [8, 9]. Unfortunately, despite this simple method for removing Fe, it has not been widely evaluated whether Fe can be consistently removed via pH control under various EAFD and acid leaching conditions.

Herein, we investigated the characteristics of EAFD that could affect Zn leaching and the acid leaching conditions that could allow the effective recovery of Zn while minimizing Fe leaching from EAFD at room temperature and atmospheric pressure. The effects of the physicochemical properties (elemental composition, crystallinity, grain size, and morphology) of four different EAFDs on acid leaching were compared. The effects of operating factors such as acid type (H_2SO_4, HCl), acid concentration, L/S ratio, and leaching time on the leaching behavior of Zn and Fe were also investigated as a function of pH. The main objective of this study was to identify specific properties of EAFD that will give consistent and high Zn recovery rates, allowing efficient operation of acid leaching process, and to confirm that pH can be used as a process control parameter to attain consistent leaching of Zn without Fe from various EAFDs in an acid leaching process.

2. Materials and Methods

Four EAFD samples ($EAFD_1$, $EAFD_2$, $EAFD_3$, and $EAFD_4$) were obtained from 'H' steel mill (Dangjin, Chungnam Province, South Korea) and used as received. The EAFDs were collected at appropriate time intervals from the same electric steelmaking furnace and fully dried in air before use. For comparison, Zn oxide (ZnO, Sigma-Aldrich Co.), $ZnFe_2O_4$ (50 nm, Aladdin Industrial Co.), and Fe oxide (Fe_2O_3, Fe_3O_4, Sigma-Aldrich Co.) reagents were used.

For elemental analyses, the EAFDs (0.1 g) were dissolved by ultrasonic acid dissolution (MARS 6, CEM Co.) using 100 mL of an acid solution prepared by adding 5 mL each of HNO_3, HCl, HF, and aqua regia, followed by digestion under microwave irradiation at 210℃ for 60 min [4, 15]. Elemental compositions were

determined by inductively coupled plasma mass spectrometry (ICP-MS; iCAP-Q, Thermo Fisher Scientific). The mineralogical phase of each EAFD was analyzed by X-ray diffraction (XRD; Cu-K, DE/D8 Advance, Bruker Co.) at 40 kV and 40 mA, and the XRD peaks were assigned using the EVA library (Version 3.0, Bruker Co.). Particle size analysis was performed using a laser scattering particle size analyzer (Mastersizer 3000, Malvern Co.). Scanning electron microscopy with energy-dispersive spectrometry (SEM-EDS; SU8010, Hitachi Co.) was used to identify the mineralogical species and morphologies of the EAFDs and acid leaching residues.

Two-way analysis of variance (ANOVA) was used to evaluate the interactive effects of the Fe-to-Zn ratio (Fe/Zn, w/w) and the specific particle size (d_{50}) on Zn extraction from the EAFDs and to characterize the EAFDs that offer a high rate of Zn recovery at room temperature under normal pressure, irrespective of the other conditions. ANOVA was implemented on 17 data points, including published results (Table 1), using the SPSS statistics program (Version 18.0). Here, the Zn extraction levels (%) refer to the maximum extractable Zn content (from both ZnO and $ZnFe_2O_4$) in the EAFD by H_2SO_4 leaching under the optimized conditions (L/S ratio, acid concentration, and leaching time) at room temperature and under normal pressure. The variances and their levels, which were assigned by referring to the empirical data, are assigned to Fe/Zn ratio of 3 levels (≤ 1; $1 <$ Fe/Zn ratio ≤ 3; $3 <$) and particle size of 2 levels (≤ 5; $5 <$).

Acid leaching experiments were performed as batch experiments in a 0.5 L Pyrex reactor vessel with an L/S ratio of 3 and a stirring rate of 300 rpm, which were set based on our preliminary results and related literature results on the acid leaching of EAFD [6] under constant temperature and pressure (20℃, 1.0 atm). Leaching experiments with varying leaching times (0-120 min), L/S ratios (1-10 mL/g), acid types (H_2SO_4, HCl), and acid concentrations (0-3 mol/L H_2SO_4, 0-4 mol/L HCl) were conducted in 100 mL of acid solution. Small aliquots (5 mL) taken at regular time intervals were immediately filtered using a cellulose acetate filter (0.2 μm, Adventec) to remove residual particles. Zn and Fe in the leachates were diluted with 1% aqueous HNO_3 and analyzed by atomic absorption spectrometry (AAS; Solaar M6, Thermo Scientific). The pH of the leachate was measured using a pH meter (Orion Star A211, Thermo Scientific) after filtration. Residual EAFDs after leaching were washed with water 2-3 times and collected by centrifugation (10,000 rpm, Hanil SUPRA 25K). After drying at 105℃, the residues were analyzed using XRD and SEM-EDS.

3. Results and Discussion

3.1. Physicochemical Properties of EAFDs

To establish the differences between the four EAFDs used in this study, the elemental compositions, particle size distributions, and Zn extraction levels were examined (Table 1). Literature values are also included for comparison. Both the Zn and Fe contents in $EAFD_{1-4}$ were 10-30%, while the calcium and lead contents were 2-10% and 0.2-2%, respectively. The Fe/Zn ratios in $EAFD_1$ and $EAFD_2$ were 0.81 and 0.72, respectively. $EAFD_3$ and $EAFD_4$

Table 1. Chemical Compositions and Particle Size Distributions of Various EAFDs and the Zn Extraction Rates (%) Achieved Using H_2SO_4 Leaching
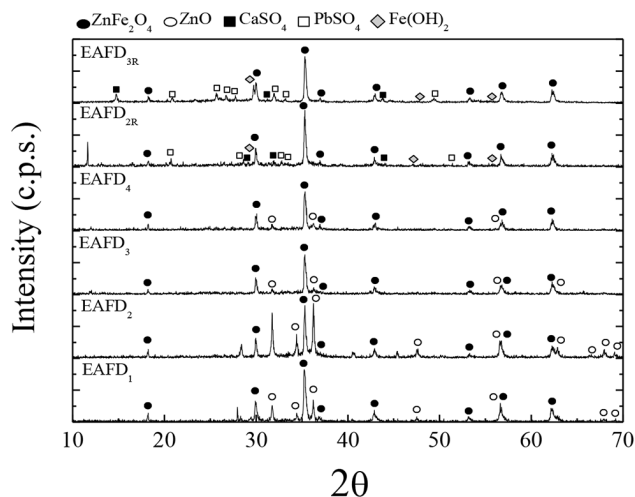
Sample	Content (%)					LOI[a]	Particle size distribution (μm)				Fe/Zn ratio	Zn extraction (%)[c]	Leaching conditions[d]	Reference
	Fe	Zn	Ca	Pb	Cd		d_{10}[b]	d_{50}	d_{90}	Mean				
$EAFD_1$	21.05	26.13	2.21	1.81	0.06	3.00	0.67	3.15	32.10	10.67	0.81	97		This study
$EAFD_2$	12.53	17.38	3.84	0.67	< 0.01	2.76	0.78	4.48	34.00	11.41	0.72	99	2 mol/L, L/S 3, 30 min	
$EAFD_3$	25.92	16.23	4.53	0.92	< 0.01	5.71	4.15	16.60	145.0	50.53	1.61	76		
$EAFD_4$	28.84	13.33	10.82	0.26	< 0.01	0.49	0.69	2.62	36.50	10.84	2.16	80		
$ZnFe_2O_4$	46.31	27.14	-	-	-	-	1.05	16.00	48.70	19.68	1.71	40	1 mol/L, L/S 5, 30 min	
$EAFD_{(a)-1}$	49.10	3.54	8.40	0.51	-	2.82	-	20.07	-	-	13.87	28		
$EAFD_{(a)-2}$	35.10	19.76	1.42	3.02	-	8.75	-	4.06	-	-	1.78	58		
$EAFD_{(a)-3}$	48.75	10.85	0.90	0.94	-	2.42	-	3.55	-	-	4.49	41	1 mol/L, L/S 10, 75 min	[10]
$EAFD_{(a)-4}$	39.20	14.49	1.78	1.51	-	2.56	-	3.91	-	-	2.71	49		
$EAFD_{(a)-5}$	29.79	27.07	0.90	2.55	-	9.77	-	4.38	-	-	1.10	69		
$EAFD_{(b)}$	27.80	20.90	4.30	2.70	0.03	12.18	-	-	-	-	1.33	50	0.4 mol/L, L/S 30, 60 min	[9]
$EAFD_{(c)}$	26.50	33.00	0.90	2.17	0.30	-	0.21	0.85	8.07	2.83	0.80	70	1 mol/L, L/S 12.5, 10 min[e]	[23]
$EAFD_{(d)}$	17.33	20.32	13.29	5.59	0.04	6.45	0.25	19.30	102.80	-	0.85	77	1.5 mol/L, L/S 10[e]	[24]
$EAFD_{(e)}$	45.00	8.00	3.70	2.10	0.04	-	-	-	-	-	5.63	60	0.3 mol/L, L/S 50, 100 min	[7]
$EAFD_{(f)}$	24.00	29.10	3.16	3.64	0.11	-	-	-	-	-	0.80	72	0.1 mol/L, L/S 50, 48 h[e]	[25]
$EAFD_{(g)}$	14.40	27.05	13.32	3.81	0.05	-	0.25	19.30	102.80	-	0.53	73	2.5 mol/L, L/S 3, 20 min	[8]
$EAFD_{(h)}$	27.23	17.05	4.42	1.28	0.09	7.08	3.00	25.00	50.00	-	1.60	60	1 mol/L, L/S 20, 60 min	[6]
$EAFD_{(i)}$	27.39	26.95	2.49	3.75	0.12	-	-	-	-	-	1.02	79	1.6 mol/L, L/S 30, 50 min	[26]
$EAFD_{(j)}$	14.40	22.73	13.32	4.22	0.09	-	0.25	19.30	102.80	-	0.63	74	1 mol/L, L/S 5, 20 min	[17]
$EAFD_{(k)-1}$	23.00	8.00	10.00	0.30	0.10	-	-	24.00	-	-	2.88	46	0.5 mol/L, L/S 10[e]	[27]
$EAFD_{(k)-2}$	20.00	6.00	13.00	1.00	0.30	-	-	22.00	-	-	3.33	33		

[a] LOI: Loss of ignition.
[b] d-values from the intercept for 10%, 50%, and 90% of the cumulative mass.
[c] Maximum Zn extraction rate under ambient conditions (20°C, 1 atm).
[d] Optimized leaching conditions for maximum Zn extraction.
[e] Performed at 30-40°C.

exhibited markedly higher Fe/Zn ratios of 1.61 and 2.16, respectively. A high Fe/Zn ratio increases the possibility that Zn will react with Fe oxide during high-temperature smelting to form $ZnFe_2O_4$ [5, 10]. To confirm this, the XRD patterns of $EAFD_{1-4}$ were compared (Fig. 1). In $EAFD_{1,2}$, the $ZnFe_2O_4$ and ZnO peak intensities were similar. By contrast, $EAFD_{3,4}$, with relatively high Fe content, exhibited a higher peak intensity for $ZnFe_2O_4$ than for ZnO. In previous studies, EAFDs with a high Fe/Zn ratio ($EAFD_{(h)}$, Table 1) exhibited a high-intensity $ZnFe_2O_4$ peak similar to that observed for $EAFD_{3,4}$, whereas EAFDs with a low Fe/Zn ratio ($EAFD_{(d,e,f)}$, Table 1) displayed XRD patterns similar to those of $EAFD_{1,2}$. Thus, higher Fe/Zn ratios correspond to a higher fraction of Zn existing in its mineralogical form, i.e., $ZnFe_2O_4$, in the EAFD. Similarly, Machado et al. [15] determined using Mössbauer spectroscopy that EAFDs with Fe/Zn ratios of 5.3 contain 15 times more $ZnFe_2O_4$ than ZnO.

The mean particle size of $EAFD_1$ and its d_{50} value (the median diameter) were 10.67 μm and 3.15 μm, respectively (Fig. 2). The mean particle size of $EAFD_2$ (11.41 μm) was similar to that of $EAFD_1$. By contrast, $EAFD_3$ displayed a larger particle size distribution (d_{50} = 16.60 μm), with a mean particle size of 50.53 μm. The mean particle size of $ZnFe_2O_4$ and its d_{50} values were 19.68 μm and 16.00 μm, respectively, very similar to the values for $EAFD_3$. These results agree well with the results of the elemental and mineralogical phase analysis, indicating that an EAFD with a high $ZnFe_2O_4$ content may have a relatively large particle size distribution [2, 16]. Similarly, Montenegro et al. [8] used SEM analysis to show that ZnO in EAFD is mainly present as fine particles, while spinel-type $ZnFe_2O_4$ adopts larger spherical particles. Further, Suetens et al. [12] noted that EAFD particles of < 1 μm are composed mostly of ZnO.

SEM-EDS analyses of $EAFD_1$ and $EAFD_3$ revealed that the mineralogical phases and morphologies (Fig. 3) differed depending on the Fe/Zn ratio. The EAFD particles were mostly spherical with various sizes, and notably, $EAFD_1$ (Fe/Zn ratio < 1) had more spherical-shaped particles covered by fine particles
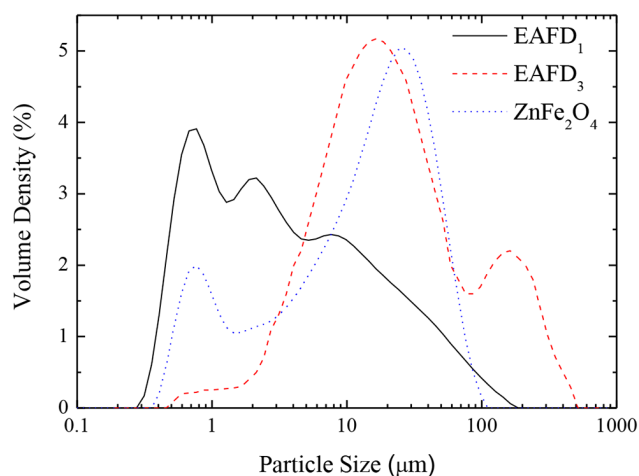
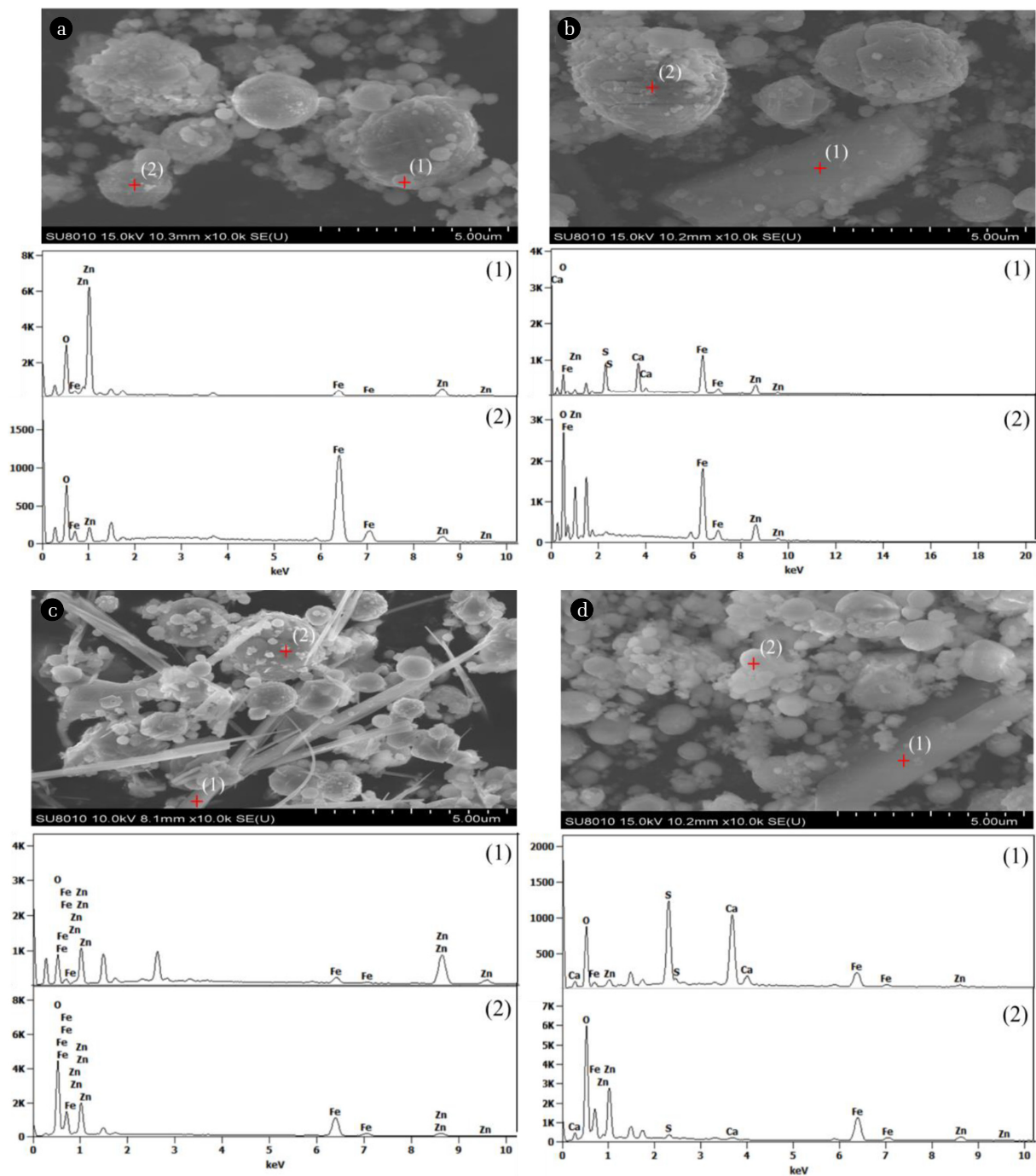
Fig. 2. Particle size distributions of EAFD samples and zinc ferrite reagent.

than $EAFD_3$ (Fe/Zn ratio > 1). In $EAFD_1$ (Fig. 3(a)), $ZnFe_2O_4$ existed as relatively large spherical crystals covered in small spherical crystals of ZnO. Interestingly, ZnO in $EAFD_3$ instead appeared as needle-shaped particles. These results were confirmed by SEM-EDS mapping (Fig. 4). The SEM image of ZnO reveals that various crystal shapes were generated depending on the ZnO generation conditions. Meanwhile, the $ZnFe_2O_4$ crystals in $EAFD_3$ were large and spherical with relatively smooth surfaces not covered in fine particles. These results agree well with the morphologies of EAFD particles reported previously [15, 17].

3.2. The Relationship between Fe/Zn Ratio, d_{50}, and Zn Extraction Rate

To investigate the main characteristics of EAFDs that affect Zn extraction, ANOVA was performed using the Fe/Zn ratio and d_{50}, which are considered closely related to the $ZnFe_2O_4$ contents of the EAFDs, as the independent factors (Table 2). The F-value of the Fe/Zn ratio with respect to the Zn extraction rate was 12.26 at the 99% confidence level ($p < 0.005$). By contrast, for d_{50}, the F-value was as low as 2.42 with high p-values (0.148). High F-values and low p-values ($p < 0.05$) indicate statistically significant variation. Thus, Zn extraction under the tested conditions was highly affected by the Fe/Zn ratio of the EAFD but not by the particle size. The average Zn extraction rates were 81.7% ± 5.3% (95% confidence interval; 70.0-93.3%) at Fe/Zn ratios < 1, 59.8% ± 4.6% (95% confidence interval; 49.6-69.7%) at Fe/Zn ratios of 1-3, and 35.8% ± 8.0% (95% confidence interval; 18.2-53.3%) at Fe/Zn ratios > 3. The high correlation between the Fe/Zn ratio and the maximum Zn extraction rate could be affected by different crystal formation mechanisms depending on the Fe/Zn ratio. Suetens et al. [12] suggested two $ZnFe_2O_4$ formation mechanisms: a solid-solid reaction and a gas-solid reaction. The relatively large amount of Zn in EAFD with a low Fe/Zn ratio increases the possibility that ZnO crystals are generated and precipitated on the surface of the Fe oxide. Through a solid-solid reaction between the two oxides, EAFD with a low Fe/Zn ratio is expected to form large spherical crystals covered by fine ZnO particles, with $ZnFe_2O_4$ formed on the outer surfaces of the spherical Fe oxide crystals

**Fig. 1.** XRD patterns of $EAFD_{1-4}$ and their residues (denoted by 'R') after acid leaching (0.5 mol/L H_2SO_4, L/S ratio = 3, reaction time = 30 min, 20℃).

Fig. 3. SEM images and EDS spectra of (a) EAFD$_1$, (b) leached residue of EAFD$_1$, (c) EAFD$_3$, and (d) leached residue of EAFD$_3$.

(Fig. 3(a)). As confirmed by SEM-EDS mapping (Fig. 4), Zn exists on the outer surface of the spherical particles. In contrast, the relatively high Fe content of EAFD with a high Fe/Zn ratio allows Zn vapor to react directly through a gas-solid chemical diffusion reaction to form the spinel phase. By this mechanism, Zn was observed homogeneously throughout the entire crystal (Fig. 4). Consequently, EAFD with a low Fe/Zn ratio could have a large amount of ZnO crystals that dissolve more easily than ZnFe$_2$O$_4$ during acid leaching, and ZnFe$_2$O$_4$ can easily be exposed to the acid, resulting in a high Zn extraction rate. By contrast, the lack of a statistically significant relationship between Zn extraction and d_{50} can be explained by EAFD particle aggregation, induced by exposure to air moisture, which can distort the actual particle sizes such as in EAFD$_3$ [10].
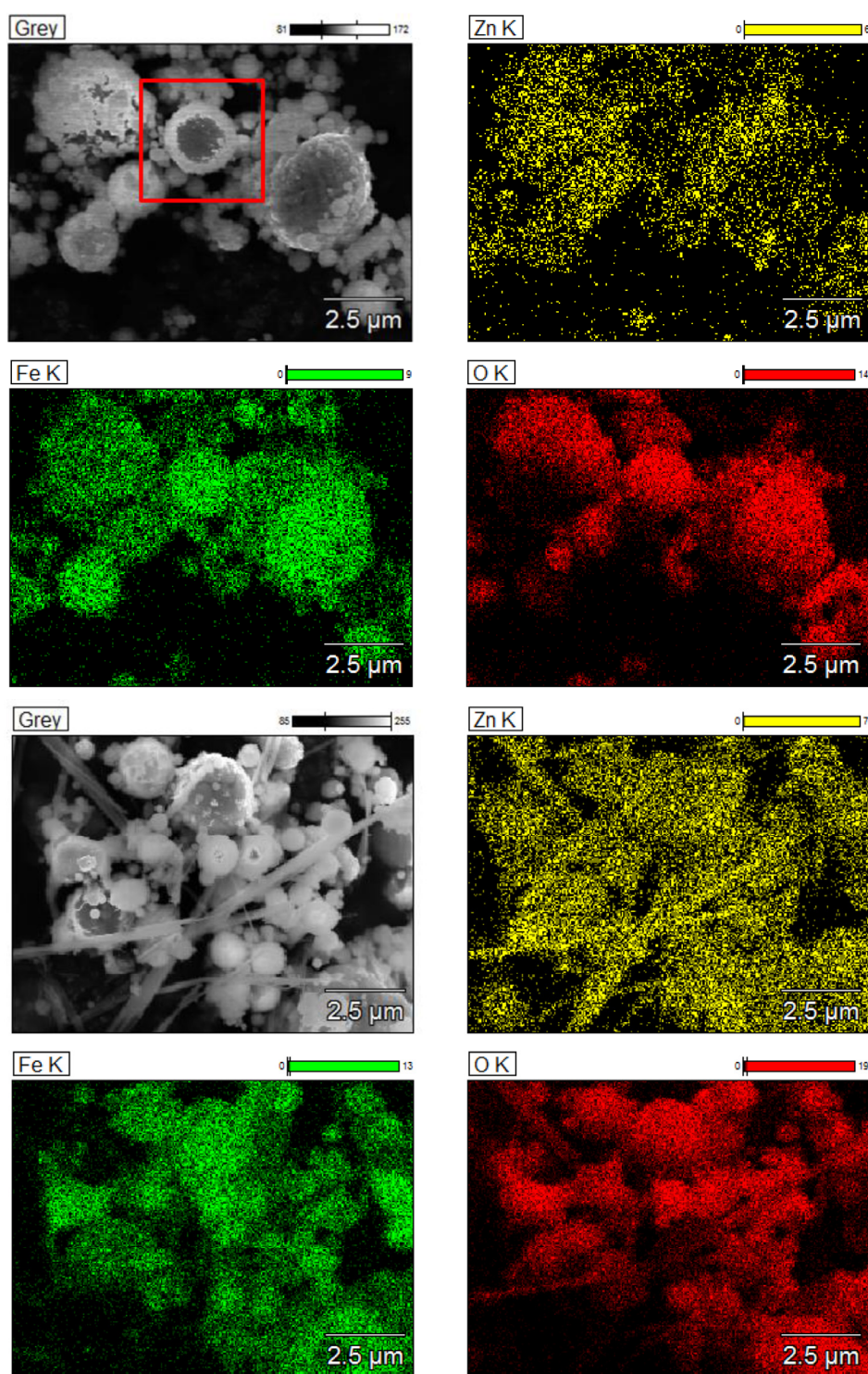
Fig. 4. SEM-EDS mapping results for $EAFD_1$ (up) and $EAFD_3$ (down).

The ANOVA results showed that a high Fe/Zn ratio was significantly correlated with a high $ZnFe_2O_4$ content in EAFDs and a low Zn extraction rate. That is, the lower the Fe/Zn ratio in the EAFD, the lower the $ZnFe_2O_4$ content in the sample and the higher the Zn extraction rate that can be obtained. Thus, it might be possible to use the Fe/Zn ratio as a screening factor to select EAFDs for high Zn recovery via acid leaching under ambient conditions.

Table 2. Summary of ANOVA Results to Evaluate the Influence of Fe/Zn Ratio and Specific Particle Size (d50) on Zn Recovery from EAFDs Using Acid Leaching under Ambient Conditions (20°C, 1 atm)
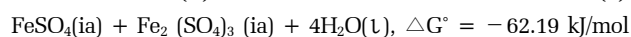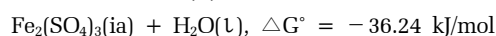
Source	Sum of squares	Degrees of freedom	Mean square	F	Sig.
Fe/Zn ratio	4,144.667	2	2,072.333	12.263	0.002
Specific particle size (d_{50})	408.375	1	408.375	2.417	0.148
Fe/Zn ratio specific particle size (d_{50})	26.000	2	13.000	0.077	0.926

3.3. Effect of Acid Leaching Time and L/S Ratio on pH and Metal Leaching

During leaching, the acid is consumed by reaction with the metal oxides in the EAFD, resulting in a change in the pH. Thus, the changes in pH and the dissolution behaviors of Zn and Fe from the EAFDs were investigated as a function of leaching time and L/S ratio (mL/g). Fig. 5(a) shows the changes in the extraction of Zn and Fe from $EAFD_1$ subjected to acid leaching in 1.4 mol/L H_2SO_4 at 20°C and an L/S ratio of 3 for 1 h. Zn leaching proceeded very quickly compared with Fe leaching, with ~80% of the total Zn content leached within 5 min. This result was attributed to the high acid solubility of ZnO, which is present in the form of fine particles. By contrast, the low initial leaching rate of Fe (~5%) decreased further to < 0.5% after 30 min. These results could be explained by the Gibbs free energy (ΔG°, 20°C, 1 atm) of the main oxide components, as given in Eq. (1)-(4) [9]. That is, the more rapid consumption of added acid by ZnO than by Fe oxides in the EAFD stems from the high negative ΔG° value for the ZnO reaction, whereas Fe oxides and $ZnFe_2O_4$ have relatively low acid solubilities. The pH of the leaching solution increased sharply from 2 to 4.5 over the initial 30 min through consumption of the acid or its reaction with a metal oxide (e.g., ZnO). As the leaching time elapsed, the leached Fe was converted into Fe(III) hydroxide ($Fe(OH)_3$) owing to the increased solution pH (> 4.5) induced by the acid dissolution of metal oxides (i.e., basic anhydrate) [6]. Trivalent Fe (Fe^{3+}) is produced from $ZnFe_2O_4$ by acid leaching (Eq. (4)), and we confirmed that it mostly precipitates as $Fe(OH)_3$ at pH > 4.5 using Visual MINTEQ 3.1. Similar results were observed for the EAFDs examined in this study (data not shown), suggesting that leaching of Zn with minimum Fe dis-

solution is possible when the pH is maintained above 4.5 by adjusting the leaching time [7].

Zn and Fe exhibited similar changes in leaching behavior as a function of pH (Fig. 5(b)) when the L/S ratio (mL/g) was varied. Specifically, at an L/S ratio of 3 with the solution pH maintained at 4.5, selective Zn extraction (> 90%) with minimum Fe dissolution was achieved. However, when the L/S ratio was increased to > 4, the solution pH decreased to < 2, and 8-10% of Fe was dissolved.

$$ZnO + H_2SO_4(l) \rightleftharpoons \tag{1}$$
$$ZnSO_4(a) + H_2O(l), \triangle G° = -134.57 \text{ kJ/mol}$$

$$Fe_2O_3 + 3H_2SO_4(l) \rightleftharpoons \tag{2}$$
$$Fe_2(SO_4)_3(ia) + H_2O(l), \triangle G° = -36.24 \text{ kJ/mol}$$

$$Fe_3O_4 + 4H_2SO_4(l) \rightleftharpoons \tag{3}$$
$$FeSO_4(ia) + Fe_2(SO_4)_3(ia) + 4H_2O(l), \triangle G° = -62.19 \text{ kJ/mol}$$

$$ZnFe_2O_4 + 4H_2SO_4(l) \rightleftharpoons \tag{4}$$
$$ZnSO_4(ia) + Fe_2(SO_4)_3(ia) + 4H_2O(l), \triangle G° = -67.07 \text{ kJ/mol}$$

### 3.4. Effect of Acid Concentration on pH and Metal Leaching

The effect of acid concentration (0-3 mol/L) on the leaching efficiencies of Zn and Fe was studied under constant conditions (L/S = 3, leaching time = 30 min, temperature = 20°C) (Fig. 6). To evaluate the effect of leaching time, the results obtained at a leaching time of 5 min are also presented in Fig. 6. The leaching rate of Zn increased sharply from 5.8% to 92% as the acid concentration
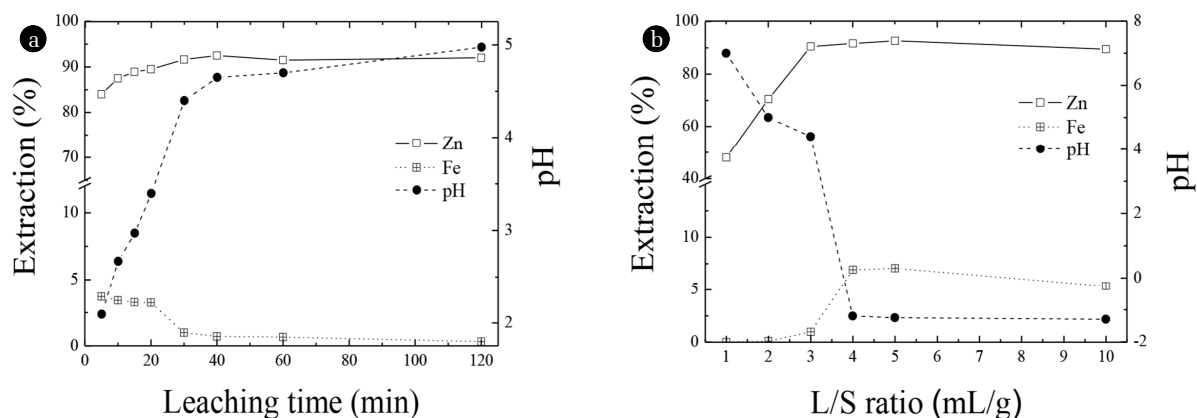
Fig. 5. Changes in metal extraction and pH as a function of (a) leaching time and (b) L/S ratio for EAFD1 in 1.4 mol/L H_2SO_4 at 20°C. The leaching time for experiment (b) was 30 min.

increased from 0.1 to 1.4 mol/L, and reached the maximum leaching rate (> 97%) at an acid concentration of 2.0 mol/L. Selective leaching of Zn without Fe dissolution was observed at pH 4.6. Fe was not dissolved until the acid concentration reached 1.4 mol/L, and the leaching rate was low (~10%) even under strongly acidic conditions (3.0 mol/L). This behavior occurs because ZnO in the EAFD is dissolved easily in the acid solution, whereas the dissolution of Fe components such as Fe oxide and $ZnFe_2O_4$ is quite low (Eq. (1)-(4)). These results were corroborated by the fact that the maximum recoveries (2.0 mol/L H_2SO_4, pH < 0) of Zn and Fe from $EAFD_{3,4}$, which contain higher contents of $ZnFe_2O_4$, were lower than those from $EAFD_1$ (Zn: 80% *vs.* 98%, Fe: < 5% *vs.* 11%). To verify these results, acid leaching experiments were performed for Fe oxides, ZnO, and $ZnFe_2O_4$ under similar conditions (Table 1, 1.4 mol/L H_2SO_4, L/S = 5, 20°C). ZnO was extracted very quickly (< 5 min) with a recovery of > 93%, while $ZnFe_2O_4$ showed relatively low extraction (Zn: 40%, Fe: 18%). Notably, hematite (Fe_2O_3) and magnetite (Fe_3O_4) showed no acid solubility under the tested leaching conditions (data not shown), suggesting that the leaching of Fe from the EAFDs occurs mostly via the partial dissolution of the $ZnFe_2O_4$ components.

Examination of the effect of leaching time (Fig. 6) revealed that Fe in the leachate can be reprecipitated by increasing the pH from 2.7 to 4.5 (at H_2SO_4 = 1.4 mol/L) with an increase in the leaching time from 5 to 30 min. The extraction rate of Zn also increased from 80% to 92% under these conditions. Thus, to obtain a high Zn recovery rate without Fe leaching, the solution pH should be maintained at > 4.5 by adjusting the acid amount and the reaction time, as previously confirmed by the results shown in Fig. 5.
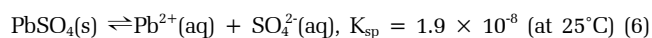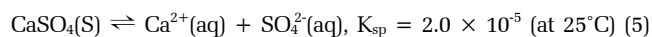
Regardless of the properties of the EAFDs and the acid type used, a pH of > 4.5 ensured the highest extraction of Zn while minimizing Fe leaching. Decreasing the pH of the leaching solution from ~4.6 to < 0 by increasing the acid concentration to 2 mol/L H_2SO_4 increased the Zn recovery rates of $EAFD_{1-4}$ from ~2% to
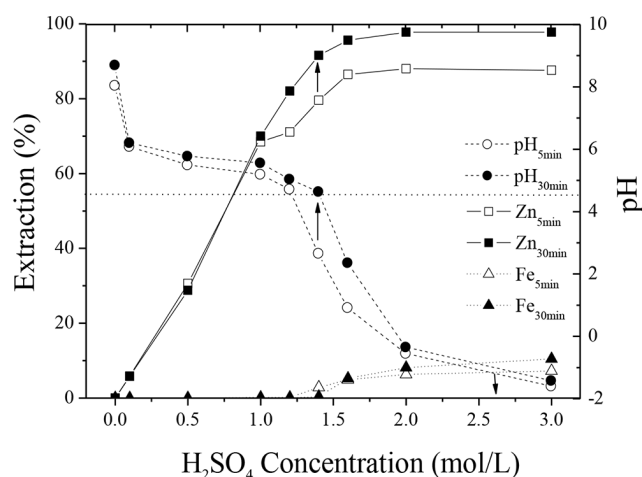
10%, but the Fe dissolution levels increased from 1.5% to 8.1%. The leaching behaviors of Zn and Fe as a function of pH were similar when HCl was used under the same reaction conditions (L/S = 3, reaction time = 30 min, 300 rpm) [18]. The optimum HCl concentration for leaching of Zn with minimum Fe dissolution was 1.2 mol/L, corresponding to a solution pH of 4.9 (data not shown). These results suggest that the pH of the leaching solution can be used as a process control factor to facilitate the leaching of Zn without Fe, irrespective of the type of acid used and the properties of the EAFDs [19-21]. In particular, Behnajady and Moghaddam [19], who studied the effects of various parameters (temperature, reaction time, L/S ratio, stirring speed, and pH) on the extraction of metals from a Zn plant hot purification filter cake, reported that the pH had the strongest effect on the selective leaching of Zn. On the other hand, the concentrations of lead and cadmium in the acid leaching solution of $EAFD_{1-4}$ were very low (0.3-0.7 mg/L and ND (not detected)-0.3 mg/L, respectively, as determined by ICP-MS), and the metals remaining in solution could be removed by subsequent Zn refining, which is commonly performed by reductive precipitation using Zn powder [6].

Furthermore, Fig. 1 shows the XRD patterns of the residues of $EAFD_2$ and $EAFD_3$ separated from the leaching solution after reaction at pH 4.5 (reaction time = 30 min, L/S = 3, temperature = 20°C). No ZnO peak was observed in the XRD patterns of the leached residues, whereas the $ZnFe_2O_4$ peak intensity for the leached residues increased relative to that for the EAFDs before acid leaching. An $Fe(OH)_3(s)$ peak was only observed for the leached residues, but the peak intensity was low owing to the very small amount of Fe dissolved from the EAFD. $CaSO_4(s)$ and $PbSO_4(s)$ peaks were also observed, which may be attributed to the reaction of Ca and Pb ions in the EAFDs with H_2SO_4 (Eq. (5) and (6)). Further, the SEM-EDS results for the leached residues (Fig. 3(c) and 3(d)) indicated that $ZnFe_2O_4$ consisted of spherical particles of various sizes, whereas $CaSO_4$ consisted of needle-like crystals of 5-10 μm in length and 1-2 μm in diameter [22]. The ZnO crystals disappeared owing to total dissolution during acid leaching. However, $Fe(OH)_3$ and $PbSO_4$ crystals were difficult to identify by SEM-EDS owing to their very low contents in the leached residues.

$$CaSO_4(S) \rightleftharpoons Ca^{2+}(aq) + SO_4^{2-}(aq), K_{sp} = 2.0 \times 10^{-5} \text{ (at 25°C) (5)}$$

$$PbSO_4(s) \rightleftharpoons Pb^{2+}(aq) + SO_4^{2-}(aq), K_{sp} = 1.9 \times 10^{-8} \text{ (at 25°C) (6)}$$

4. Conclusions

We investigated the main characteristics of EAFDs that yielded a high Zn recovery rate and a suitable pH range for selective Zn leaching via the acid leaching process. Comparative analysis of the physicochemical properties of the EAFDs revealed that an Fe/Zn ratio of < 1 indicates a lower content of $ZnFe_2O_4$ than of ZnO and a smaller particle size distribution. The ANOVA results showed a significant correlation between the Fe/Zn ratio and the Zn extraction rate ($p < 0.005$); in samples with an Fe/Zn ratio < 1, the mean Zn extraction rate was 81.7% ± 5.3%. Hence,

Fig. 6. Changes in metal extraction and pH with respect to time (5 or 30 min) and initial H_2SO_4 concentration for $EAFD_1$ at 20°C and an L/S ratio of 3.

EAFDs with a low Fe/Zn ratio could have a larger amount of ZnO crystals, which easily dissolve during acid leaching, than ZnFe$_2$O$_4$; further, the morphological structure of the ZnFe$_2$O$_4$ in EAFD particles can be easily exposed to the acid, resulting in a high Zn extraction rate under mild leaching conditions. On the other hands, it also confirmed that Zn can be selectively leached with minimum Fe dissolution by controlling the pH at > 4.5 with an appropriate acid amount and time, regardless of the other acid leaching conditions or the properties of the EAFDs. Thus, pH can be used as a useful operating factor to achieve selective recovery of Zn from various EAFDs without further Fe leaching. Considering the fact that EAFDs containing a large amount of acid-insoluble Zn ferrite require harsh leaching condition (e.g., high temperature and pressures) to obtain high Zn recovery, the pre-selection of EAFDs based on their Fe/Zn ratios and the application of pH control during acid leaching will assure such a high Zn recovery in a mild leaching condition and/or even under ambient conditions by separating the Zn ferrites with high Fe content, which can provide a more economical Zn recovery process.

Acknowledgments

References

1. Wu S, Chang F, Zhang J, Lu H, Kou M. Cold strength and high temperature behaviors of self-reducing briquette containing electric arc furnace dust and anthracite. *ISIJ Int.* 2017;57:1364-1373.

2. Lanzerstorfer C. Electric arc furnace (EAF) dust: Application of air classification for improved Zn enrichment in in-plant recycling. *J. CLEAN Prod.* 2018;174:1-6.

3. Sofilić T, Rastovčan-Mioč A, Cerjan-Stefanović Š, Novosel-Radović V, Jenko M. Characterization of steel mill electric-arc furnace dust. *J. Hazard. Mater.* 2004;109:59-70.

4. Kelebek S, Yörük S, Davis B. Characterization of basic oxygen furnace dust and Zn removal by acid leaching. *Miner. Eng.* 2004;17:285-291.

5. de Buzin PJWK, Heck NC, Vilela ACF. EAF dust: An overview on the influences of physical, chemical and mineral features in its recycling and waste incorporation routes. *J. Mater. Res. Technol.* 2017;6:194-202.

6. Kukurugya F, Vindt T, Havlík T. Behavior of Zn, Fe and calcium from electric arc furnace (EAF) dust in hydrometallurgical processing in sulfuric acid solutions: Thermodynamic and kinetic aspects. *Hydrometallurgy* 2015;154:20-32.

7. Langová Š, Matýsek D. Zn recovery from steel-making wastes by acid pressure leaching and hematite precipitation. *Hydrometallurgy* 2010;101:171-173.

8. Montenegro V, Oustadakis P, Tsakiridis PE, Agatzini-Leonardou S. Hydrometallurgical treatment of steelmaking electric arc furnace dusts (EAFD). *Metall. Mater. Trans. B* 2013;44:1058-1069.

9. Havlik T, Turzakova M, Stopic S, Friedrich B. Atmospheric leaching of EAF dust with diluted sulphuric acid. *Hydrometallurgy* 2005;77:41-50.

10. Mantovani MC, Takano C, Büchler PM. EAF and secondary dust characterisation. *Femak. Steelmak.* 2004;31:325-332.

11. Havlik T, Maruskinova G, Miskufova A. Determination of ZnO amount in electric arc furnace dust and temperature dependence of leaching in ammonium carbonate by using of X-ray diffraction. *Arch. Metall. Mater.* 2018;63:653-658.

12. Suetens T, Guo M, Van Acker K, Blanpain, B. Formation of the ZnFe$_2$O$_4$ phase in an electric arc furnace off-gas treatment system. *J. Hazard. Mater.* 2015;287:180-187.

13. Tsakiridis PE, Oustadakis P, Katsiapi A, Agatzini-Leonardou S. Hydrometallurgical process for Zn recovery from electric arc furnace dust (EAFD). Part II: Downstream processing and Zn recovery by electrowinning. *J. Hazard. Mater.* 2010;179:8-14.

14. Zhang D, Zhang X, Yang T, et al. Selective leaching of Zn from blast furnace dust with mono-ligand and mixed-ligand complex leaching systems. *Hydrometallurgy* 2017;169:219-228.

15. Machado JGMS, Brehm FA, Moraes CAM, dos Santos CA, Vilela ACF, da Cunha JBM. Chemical, physical, structural and morphological characterization of the electric arc furnace dust. *J. Hazard. Mater.* 2006;B136:953-960.

16. Oustadakis P, Tsakiridis PE, Katsiapi A, Agatzini-Leonardou S. Hydrometallurgical process for Zn recovery from electric arc furnace dust (EAFD). Part I: Characterization and leaching by diluted sulphuric acid. *J. Hazard. Mater.* 2010;179:1-7.

17. Sekula R, Wnek M, Selinger A, Wrobel M. Electric arc furnace dust treatment: investigation on mechanical and magnetic separation methods. *Waste Manage. Res.* 2001;19:271-275.

18. Langová Š, Leško J, Matýsek D. Selective leaching of Zn from Zn ferrite with hydrochloric acid. *Hydrometallurgy* 2009;95:179-182.

19. Behnajady B, Moghaddam J. Selective leaching of Zn from hazardous as-bearing Zn plant purification filter cake. *Chem. Eng. Res. Des.* 2017;117:564-574.

20. Montenegro V, Agatzini-Leonardou S, Oustadakis P, Tsakiridis PE. Hydrometallurgical treatment of EAF dust by direct sulphuric acid leaching at atmospheric pressure. *Waste Biomass Valori.* 2016;7:1531-1548.

21. Aygun A, Dogan S, Argun ME, Ates H. Removal of sulphate from landfill leachate by crystallization. *Environ. Eng. Res.* 2019;24:24-30.

22. Li Y, Lu C, Zhang H, Li J. Experimental study on chemical activation of recycled powder as a cementitious material in mine paste backfilling. *Environ. Eng. Res.* 2015;21:341-349.

23. Havlík T, e Souza BV, Bernardes AM, Schneider IAH, Miškufová A. Hydrometallurgical processing of carbon steel EAF dust. *J. Hazard. Mater.* 2006;135:311-318.

24. Antuñano N, Cambra JF, Arias PL. Development of a combined solid and liquid wastes treatment integrated into a high purity ZnO hydrometallurgical production process from Waelz oxide. *Hydrometallurgy* 2017;173:250-257.

25. Shawabkeh RA. Hydrometallurgical extraction of Zn from Jordanian electric arc furnace dust. *Hydrometallurgy* 2010;104:61-65.

26. Kul M, Oskay KO, Şimşir M, Sübütay H, Kirgezen H. Optimization of selective leaching of Zn from electric arc fur-

nace steelmaking dust using response surface methodology. *Trans. Nonferrous Met. Soc. China* 2015;25:2753-2762.

27. Han H, Sun W, Hu Y, Tang H, Yue T. Magnetic separation of Fe precipitate from nickel sulfate solution by magnetic seeding. *Hydrometallurgy* 2015:156:182-187.